

Decoupling of a giant planet from its disk in an inclined binary system

G. Picogna¹ and F. Marzari²

¹ Institut für Astronomie und Astrophysik, Universität Tübingen, Auf der Morgenstelle 10, 72076 Tübingen, Germany
e-mail: giovanni.picogna@uni-tuebingen.de

² Dipartimento di Fisica, University of Padova, Via Marzolo 8, 35131 Padova, Italy

Received 23 March 2015 / Accepted 20 August 2015

ABSTRACT

Context. We explore the dynamical evolution of a planet embedded in a disk surrounding a star part of a binary system where the orbital plane of the binary is significantly tilted respect to the initial disk plane.

Aims. Our aim is to test whether the planet remains within the disk and continues to migrate towards the star in a Type I/II mode in spite of the secular perturbations of the companion star. This would explain observed exoplanets with significant inclination respect to the equatorial plane of their host star.

Methods. We have used two different SPH codes, VINE and PHANTOM, to model the evolution of a system star+disk+planet and companion star with time.

Results. After an initial coupled evolution, the inclination of the disk and that of the planet begin to differ significantly. The period of oscillation of the disk inclination, respect to the initial plane, is shorter than that of the planet which evolves independently after about 10^4 yr following a perturbed N-body behavior. However, the planet keeps migrating towards the star because during its orbital motion it crosses the disk plane and the friction with the gas causes angular momentum loss.

Conclusions. Disk and planet in a significantly inclined binary system are not dynamically coupled for small binary separations but evolve almost independently. The planet abandons the disk and, due to the onset of a significant mutual inclination, it interacts with the gas only when its orbit intersects the disk plane. The drift of the planet towards the star is not due to type I/II with the planet embedded in the disk but to the friction with the gas during the disk crossing.

Key words. Protoplanetary disks — Methods: numerical — Planets and satellites: formation

1. Introduction

According to observational surveys, about half of solar-type stars reside in multiple stellar systems (Raghavan et al. 2010) with the frequency declining to roughly about 30% for less massive M stars (Lada 2006). This frequency is suspected to be higher among young stars (Reipurth 2000) and the subsequent decay to the present fraction may be due to dynamical instability or gravitational encounters with other stars. The presence of circumstellar disks around both components of binaries does not seem to be strongly affected by the gravitational perturbations of the companion. Spatially resolved observations of disks in binaries in the Orion nebula cluster (Daemgen et al. 2012) suggest that the fraction of circumstellar disks around individual components of binary systems is about 40%, only slightly lower than that for single stars (roughly 50%). On one side the secondary star perturbations may lead to disk truncation (Artymowicz & Lubow 1994, 1996; Bate 2000) reducing its lifespan, on the other side the presence of a circumbinary disk may feed the truncated circumstellar disks through gas streams so that their dissipation timescale does not vary significantly compared to single stars (Monin et al. 2007) and they have a chance to form planets.

Up to date, 97 exoplanetary systems have been discovered around multiple stars (Rein 2012)¹, triggering statistical comparisons with planets around single stars (Desidera & Barbieri

2007; Roell et al. 2012). The analysis indicates that planetary masses increase for smaller stellar separation while for wide binaries the physical and orbital parameters appear very similar. In effect, planet formation in close binary configurations is a complex problem (see Thébault & Haghighipour 2014, for a review) while it is expected that for large separations the effects of the binary companion on the planet growth may be less relevant. However, if the orbit of the companion star is significantly inclined respect to the initial protostellar disk plane, which is possibly co-planar with the star equator, this may lead to important dynamical consequences on the final orbit of the planet, in particular its inclination respect to the star equator. It has in fact been suggested (Batygin 2012) that the evolution of the protoplanetary disk under the perturbations of the binary may be responsible for the observed spin-orbit misalignment of some exoplanets. According to Triaud et al. (2010) and Albrecht et al. (2012) about 40% of hot Jupiters have orbits significantly tilted respect to the equatorial plane of the star. A fundamental requirement of the model of Batygin (2012) is that the planet resides within the disk during its evolution. In this way it would continue its migration by tidal interaction with the disk and, at the same time, it will follow the inclination evolution of the disk. Once the disk is dissipated its migration will stop, while the evolution of the inclination will continue, though in a different fashion, until the binary companion is possibly stripped away leaving the planet on an inclined orbit.

¹ github.com/OpenExoplanetCatalogue/open_exoplanet_catalogue/

Previous studies seem to suggest that indeed a giant planet is forced to evolve within its birth disk even in presence of external perturbing forces. Any relative inclination between the planet and the disk plane, induced either by a planet–planet scattering event or by resonances (Thommes & Lissauer 2003), is quickly damped by the disk leading to a realignment of the planet orbit with the disk plane (Cresswell et al. 2007; Marzari & Nelson 2009; Bitsch & Kley 2011; Rein 2012; Teyssandier et al. 2013). However, the precession rate of the planetary orbit due to the interaction with the binary star is faster than that of the disk. As a consequence, if the damping of the disk on the planet orbit is not strong enough to keep it within the disk plane, the planet will evolve independently under the secular perturbations of the secondary star and develop a significant relative inclination respect to the disk. The assumed type II migration will not occur in this case since the planet is not embedded in the disk and cannot open a gap.

In a recent paper, Xiang-Gruess & Papaloizou (2014) have investigated the evolution of a disk and massive planet under the influence of an inclined binary companion. According to their SPH simulations, the planet and disk maintain approximate coplanarity during the evolution of the system and the planet would quickly migrate towards the star and stop on a close orbit. This findings seem to confirm the model described in Batygin (2012) for small separations between the binary components. To further test these findings, we have performed numerical simulations with a setup similar to that adopted in Xiang-Gruess & Papaloizou (2014) and used two different SPH codes: VINE (Wetzstein et al. 2009; Nelson et al. 2009) and PHANTOM (Price & Federrath 2010; Lodato & Price 2010). Our runs extend over a much longer timescale and we adopted a higher resolution. The simulations show that the initial coplanarity is maintained only for a limited amount of time and that the planet definitively detaches from the disk plane as soon as the disk completes a quarter of its precession period. The secular perturbations of the binary companion in an inclined orbit overcome the damping force of the disk and the planet evolves independently of the disk. A significant mutual inclination develops between the disk and the planet orbital plane but this does not halt the orbital migration. When the planet crosses the disk it is still affected by the gas via dynamical friction and its inward drift continues even if at a slower rate compared to that computed by Xiang-Gruess & Papaloizou (2014) in the initial stages of the system evolution.

In Sec. 2 we study the theoretical model of the precession rates in a star+disk+planet–star system and compare evolution timescales. In Sec. 3 we describe in detail the model setup of the numerical simulations. Then, in Secs. 4 and 5 we show the results of the long term high resolution models for different binary inclinations, and in Sec. 6 we discuss our results and their implications.

2. Relevant timescales

We compare in this section the timescales of precession of the angular momentum of the planet computed within a pure N–body problem and that estimated for the disk. This may give important hints on the forces that may try to separate the planet from the disk and give a better insight on the results of our SPH simulations. In computing the precession timescales, we consider a planet of mass M_p initially on a circular orbit around a star of mass M_\star at a semimajor axis a , with a distant binary companion of mass M_b , semimajor axis a_b , inclination i_B , and eccentricity e_b which we assume to be 0 at the beginning. The perturbations of the companion star are strong in particular for incli-

nations higher than $i_B \sim 39^\circ$ when the Kozai–Lidov mechanism (Kozai 1962; Lidov 1962) forces wide oscillations of both the inclination and eccentricity of the planet whose values are tied by the conservation of $L_z = \sqrt{(1-e^2)} \cos(i_p)$. The maximum eccentricity reachable by the planet is $e_{\max} \simeq \sqrt{1 - 5/3 \cos^2 \theta_{\text{pb}}^0}$. However, short range forces like General Relativity and tidal distortions (which we neglect here), and the dumping effect of the protoplanetary disk, tend to reduce this value.

The Kozai cycles occur at a characteristic period given by (Kiseleva et al. 1998)

$$\begin{aligned} P_{\text{KZ}} &\simeq \frac{P_b^2}{P_p} (1 - e_b^2)^{3/2} \frac{M_\star + M_b}{M_b} \\ &= \frac{2\pi}{\Omega_p} \left(\frac{a_b}{a} \right)^3 \left(\frac{M_\star}{M_b} \right) (1 - e_b^2)^{3/2} \end{aligned} \quad (1)$$

(see also Ford et al. 2000) where P_p and P_b are the orbital periods of the planet and binary. The dynamical evolution of the planet can also be viewed from the point of view of the orbital angular momentum. According to Storch et al. (2014), the planetary orbital angular momentum vector precesses around the binary axis ($\hat{\mathbf{L}}_b$) at a rate that, in the absence of tidal dissipation, is approximately given by

$$\Omega_{\text{pb}} \simeq \frac{3\pi}{2} P_{\text{KZ}}^{-1} \cos \theta_{\text{pb}}^0 \sqrt{1 - e_0^2} \left[1 - 2 \left(\frac{1 - e_0^2}{1 - e^2} \right) \frac{\sin^2 \theta_{\text{pb}}^0}{\sin^2 \theta_{\text{pb}}} \right] \quad (2)$$

where e_0 is the initial eccentricity of the planet, θ_{pb} is the inclination of the planetary orbit respect to the binary orbit, and θ_{pb}^0 is its initial value. The precession of the orbital angular momentum approximately translates into an oscillation of the planet inclination respect to the initial plane which is the disk plane. The timescales estimated by eq. 1 and 2 are then comparable.

Also the disk is affected by the binary companion gravity and the disk axis $\hat{\mathbf{L}}_d$ precesses around the binary axis $\hat{\mathbf{L}}_b$, assuming that it satisfies the condition for a coherent behavior as a solid body, with a period given by

$$\begin{aligned} P_d^{\text{prec}} &\simeq P_{\text{out}} \left(\frac{a_b}{r_{\text{out}}} \right)^3 \left(\frac{M_\star}{M_b} \right) \frac{1}{K \cos \theta_{\text{db}}} \\ &\simeq 2\pi \left(\frac{a_b^6}{GM_\star r_{\text{out}}^3} \right)^{1/2} \left(\frac{M_\star}{M_b} \right) \frac{1}{3/8 \cos \theta_{\text{db}}} \end{aligned} \quad (3)$$

(see Bate et al. 2000; Lai 2014), where r_{out} and P_{out} are the radius and Keplerian period of the outer disk edge respectively, and θ_{db} is the inclination of the disk respect to the orbital plane of the binary. The relative precession rate is given by

$$\Omega_{\text{db}} \simeq -\frac{3}{8} \left(\frac{GM_\star r_{\text{out}}^3}{a_b^6} \right)^{1/2} \left(\frac{M_b}{M_\star} \right) \cos \theta_{\text{db}} \quad (4)$$

Even in this case, the precession can be translated in a periodic oscillation of the disk inclination respect to the initial plane which can be assumed to have been the equatorial plane of the primary star.

If we now compare the two precession rates, that of the planet and that of the disk, we find that the initial ratio between them, under the assumption that the planet formed in the mid-plane of the disk ($\theta_{\text{pb}} = \theta_{\text{pb}}^0 = \theta_{\text{db}}$) in a circular orbit ($e = e_0 = 0$),

is given by

$$\begin{aligned} \left(\frac{P_d^{\text{prec}}}{P_p^{\text{prec}}}\right)_{\text{ini}} &= \left(\frac{\Omega_{\text{pb}}}{\Omega_{\text{db}}}\right)_{\text{ini}} \simeq 4\pi P_{\text{KZ}}^{-1} \left(\frac{a_b^6}{GM_\star r_{\text{out}}^3}\right)^{1/2} \frac{M_\star}{M_b} \\ &= 2 \left(\frac{a}{r_{\text{out}}}\right)^{3/2} = 2 \left(\frac{a}{a_b/3}\right)^{3/2} \end{aligned} \quad (5)$$

where in the last step we assumed that the binary truncates by tidal interaction the disk maximum radius to 1/3 of the binary separation, which is a good approximation for binary separations less than ~ 300 au (Artymowicz & Lubow 1994).

For $t \neq t_0$ and $e_0 = 0$ the ratio is evolving as

$$\frac{P_d^{\text{prec}}}{P_p^{\text{prec}}} \simeq 2 \frac{\cos \theta_{\text{lb}}^0}{\cos \theta_{\text{db}}} \left(\frac{a}{a_b/3}\right)^{3/2} \left[2 \left(\frac{1}{1-e^2}\right) \frac{\sin^2 \theta_{\text{lb}}^0}{\sin^2 \theta_{\text{lb}}} - 1\right] \quad (6)$$

If we consider a typical case of an equal mass binary made of solar-type stars on a circular orbit and separated by 100 au and a planet orbiting around the primary with $a = 5$ au and embedded in a disk with outer radius of 30 au, from eq. 5 the two period differs by about a factor ten. This is a large difference and the disk damping must overcome the tendency of the planet to evolve on a slower timescale and then out of the disk plane.

3. Model description

In this section we briefly describe the two numerical algorithms we have used to model the system planet+disk+binary companion and outline their differences which might affect long term results.

3.1. SPH codes and model setup

To model the evolution of a Jupiter-size planet embedded in the disk surrounding the primary star of an inclined binary system we have used two different SPH codes:

- *VINE* (Wetzstein et al. 2009; Nelson et al. 2009), which is a hybrid N-body/SPH code, updated to improve momentum and energy conservation as described in Picogna & Marzari (2013),
- *PHANTOM* (Price & Federrath 2010; Lodato & Price 2010), a modern SPH code which models the massive bodies as sink particles (Bate et al. 1995).

Both these codes solve the hydrodynamic equations in the Lagrangian approach by replacing the fluid with a set of particles (see Price 2012, for a review).

Equation of state— A locally isothermal equation of state, similar to that described in Pepliński et al. (2008), is adopted in all simulations

$$c_s = \frac{h_s r_s h_p r_p}{[(h_s r_s)^n + (h_p r_p)^n]^{1/n}} \sqrt{\Omega_s^2 + \Omega_p^2}, \quad (7)$$

where r_s , r_p are the distances of the fluid element from the primary star and the planet, respectively, and h_s , h_p are the circumstellar and circumplanetary disk aspect ratios. Ω_s and Ω_p are the circular Keplerian orbits of a fluid element around the star and planet, and $n = 3.5$ is a non-dimensional parameter chosen to smoothly join the equation of state near the planet ($c_s = h_p r_p \Omega_p$ for $r_p \ll r_s$) with that of a flat circumstellar disk ($c_s = h_s r_s \Omega_s$).

For the simulations in this work we choose a disk aspect ratio of $h_s = 0.037$, and a circumplanetary scale height of $h_p = 0.6$.

Accretion— *VINE* treats the stars and planet as N-bodies. The mass accretion has been modelled for the stars inside a radius of 0.5 au, but not for the planet.

In the simulations performed with the *PHANTOM* code, the planet (and stars) are all modelled as Lagrangian sink particles (Bate et al. 1995). A sink particle is evolved as an SPH particle, but it experiences only the gravitational force. A gas particle that comes within its accretion radius, $R_{\text{acc}} = 0.075$ au, can be accreted if

- it is inside the Hill sphere of the sink particle,
- its specific angular momentum is less than that required to form a circular orbit at the accretion radius,
- it is more bound to the candidate sink particle than to any other sink particle.

Viscosity— An artificial viscosity term is introduced in SPH codes in order to correctly model shock waves that inject entropy into the flow over distances that are much shorter than a smoothing length, and to simulate the evolution of viscous disks. The term broadens the shock over a small number of smoothing lengths and correctly resolves it ensuring at the same time that the Rankine-Hugoniot equations are satisfied. In this way it prevents discontinuities in entropy, pressure, density, and velocity fields.

The implementation of the viscosity term is slightly different in the two numerical codes. *VINE* adopts the standard formulation introduced by Monaghan & Gingold (1983) where, for approaching particles ($\mathbf{v}_{ab} \cdot \hat{\mathbf{r}}_{ab} \leq 0$), an artificial viscosity term is introduced in the momentum and energy equations

$$\Pi_{ab} = \begin{cases} \frac{(-\alpha c_{ab} \mu_{ab} + \beta \mu_{ab}^2)}{\rho_{ab}} & \mathbf{v}_{ab} \cdot \hat{\mathbf{r}}_{ab} \leq 0 \\ 0 & \mathbf{v}_{ab} \cdot \hat{\mathbf{r}}_{ab} > 0 \end{cases} \quad (8)$$

where μ_{ab} is a velocity divergence term

$$\mu_{ab} = \frac{h \mathbf{v}_{ab} \cdot \mathbf{r}_{ab}}{\mathbf{r}_{ab}^2 + \eta^2 h^2} \quad (9)$$

with $\eta^2 = 0.01$. This implementation conserves total linear and angular momentum and vanishes for rigid body rotation. α is the linear term (bulk viscosity) and it dissipates kinetic energy as particles approach each other to reduce subsonic velocity oscillations following a shock. β is the quadratic term (von Neumann-Richtmyer like viscosity), which converts kinetic energy to thermal energy preventing particle mutual penetration in shocks.

PHANTOM uses a more general formulation of dissipative terms (Monaghan 1997). It is built on an analogy with Riemann solvers, where the dissipative terms of conservative variables (density, specific momentum, and energy), that experience a jump across a shock front are multiplied by eigenvalues similar to signal velocities (v_{sig}). The viscosity term for the momentum equation becomes

$$\Pi_{ab} = \frac{1}{2} \frac{\alpha v_{\text{sig}} \mathbf{v}_{ab} \cdot \hat{\mathbf{r}}_{ab}}{\rho_{ab}} \quad (10)$$

where the signal velocity is given by

$$v_{\text{sig}} = \begin{cases} c_{s,a} + c_{s,b} - \beta \mathbf{v}_{ab} \cdot \hat{\mathbf{r}}_{ab} & \mathbf{v}_{ab} \cdot \hat{\mathbf{r}}_{ab} \leq 0 \\ 0 & \mathbf{v}_{ab} \cdot \hat{\mathbf{r}}_{ab} > 0 \end{cases} \quad (11)$$

Regarding the energy evolution an additional signal velocity $v_{\text{sig},u}$ is adopted, and the viscosity term is defined as

$$\left(\frac{du}{dt}\right)_{\text{diss},a} = - \sum_b \frac{m_b}{\rho_{ab}} \left[\frac{1}{2} \alpha v_{\text{sig}} (\mathbf{v}_{ab} \cdot \hat{\mathbf{r}}_{ab})^2 + \alpha_u v_{\text{sig},u} u_{ab} \right] \hat{\mathbf{r}}_{ab} \cdot \nabla_a W_{ab} \quad (12)$$

where the signal velocity for the energy jumps is chosen to be $v_{\text{sig},u} = |\mathbf{v}_{ab} \cdot \hat{\mathbf{r}}_{ab}|$ as in Wadsley et al. (2008).

In order to properly compare these two different approaches and derive a Shakura & Sunyaev–like viscosity value for the different simulations, we adopted the relations given by Meru & Bate (2012)

$$\alpha_{\text{SS}} = \frac{1}{20} \alpha \frac{h}{H} + \frac{3}{35\pi} \beta \left(\frac{h}{H}\right)^2 \quad (13)$$

for the Monaghan & Gingold (1983) formalism, and

$$\alpha_{\text{SS}} = \frac{31}{525} \alpha \frac{h}{H} + \frac{9}{70\pi} \beta \left(\frac{h}{H}\right)^2 \quad (14)$$

for the Monaghan (1997) one, where h is the averaged smoothing length, and H is the disk scale height.

The initial average value of α_{SS} for our VINE run is 0.02, similar to that in Xiang-Gruess & Papaloizou (2014). About twice larger is the α_{SS} in the PHANTOM run with an average initial value of 0.04.

Initial conditions— The scenario we have modelled includes a binary system composed of 2 equal mass stars $m_p = m_s = 1 M_\odot$. One of them (which we will call primary) harbors a protoplanetary disk with a Jupiter mass planet $M_p = 1 M_J$ embedded in it on an orbit with initial semimajor axis $a_p = 5$ au. Different inclinations between the two components of the binary has been studied, in a reference frame centered onto the primary star. The disk is modelled with 600 000 SPH particles, about 3 times the number used by Xiang-Gruess & Papaloizou (2014), and it extends from 0.5 to 30 au, with a surface density profile

$$\Sigma = \Sigma_0 r^{-0.5} \quad (15)$$

where Σ_0 is defined such as the total disk mass is $M_D = 0.01 M_\odot$.

The choice of the initial parameters are such that the disk will precess as a solid body. In fact, according to Papaloizou & Terquem (1995) and Larwood et al. (1996), the condition for this behavior is

$$P_{\text{out}}/P_d \leq H/R \quad (16)$$

In our initial setup this condition is fully satisfied since H/R is 0.037 while the ratio between ω_p/Ω_d is approximately 0.01. This is confirmed also by the calculations of Xiang-Gruess & Papaloizou (2013). As reference frame we adopt the initial plane of the disk and planet orbit while the binary orbit has different initial inclinations defined respect to this plane. The initial semimajor axis of the companion star is $a_b = 100$ au and it is set on a circular orbit.

4. Initial mutual inclination of 45°

The model where the inclination between the binary orbit and the initial disk+planet plane is 45° is assumed as standard model. The simulation with VINE was halted after 11 600 orbits of the

planet (125 000 yr) while that with PHANTOM was stopped after about half of that period (60 000 yr). The run with VINE required approximately 8 months of CPU on a 24 processor machine while that with PHANTOM 4 months on a 32 processor machine. In both simulations we find that in the first 6 000 yr the behavior is similar to that described in Xiang-Gruess & Papaloizou (2014) but, soon after, the dynamical evolution substantially changes. The inclination of the planet i_p , that initially follows closely that of the disk i_d , decisively departs from i_d and grows at a lower rate. In Fig. 2 both i_p and i_d are shown as a function of time for the run with VINE and PHANTOM. While the periodic oscillations of i_d continue with an almost unaltered frequency of about 2×10^4 yr, the planet inclination i_p grows on a much longer timescale reaching a maximum after about 8×10^4 yr. There are clear indications of interaction between the planet and the disk in particular when the two inclinations are comparable like after 2.5×10^4 , 5×10^4 etc. At these times the planet crosses the disk and it interacts with its gas particles.

There are some minor differences between the VINE and the PHANTOM models possibly related to the different handling of viscosity and accretion onto the planet. A circumplanetary disk develops in the initial phase of the run with VINE when $i_p \sim i_d$ but later on when the planet departs from the disk and periodically crosses it with high mutual inclination it is dissipated. In both simulations dynamical behavior of the planet shows a clear competition between the gravitational force of the binary and the interaction with the disk, but the binary secular perturbations finally dominate. The inclination of the planet roughly follows a pure N–body trend, shown as a dotted light–blue line in Fig. 2, even if i_p is strongly perturbed by the disk. The detachment between the planet and the disk can be seen also in Fig. 1, where a 3D rendering of the system is displayed at an optical depth of ~ 2 .

In Fig. 2 both simulations show a slow damping of the inclination oscillations, a behavior already suggested by Martin et al. (2014).

As discussed in Sec. 2, the distinct evolution of the planet and disk is related to their different precession timescales around the binary axis which translates in the inclination evolution shown in Fig. 2. As an additional indication of the different evolution of the planet respect to the disk in Fig. 3 we illustrate the evolution of the precession angle of the disk \mathbf{L}_D and planet \mathbf{L}_p angular momentum around that of the binary star \mathbf{L}_B , calculated respect to the initial orbital plane (Xiang-Gruess & Papaloizou 2014; Larwood et al. 1996)

$$\cos \beta_p = \frac{\mathbf{L}_D \times \mathbf{L}_B}{|\mathbf{L}_D \times \mathbf{L}_B|} \cdot \mathbf{u}, \quad (17)$$

where \mathbf{u} is the fixed unit reference vector for the initial orbital plane. The evolution timescale of the planet precession rate is ~ 10 times slower than that of the disk, confirming the theoretical prediction.

To test whether a potential warping of the disk due to binary perturbations is fully responsible for the decoupling of the planet from the disk in our models, as described in (Terquem 2013), we checked the disk shape every 300 planetary orbits. In Fig. 4 we show the disk evolution at different times and there is no evidence of a marked warping. In addition, we also performed a simulation where a smaller disk was considered. In Fig. 5 the PHANTOM code was used to model the evolution of a disk with the same mass as our standard disk but extending only to 15 au in radial distance. The warping for such a disk, being less affected by the binary perturbations extending well within the tidal truncation radius (Artymowicz & Lubow 1994), is expected to be

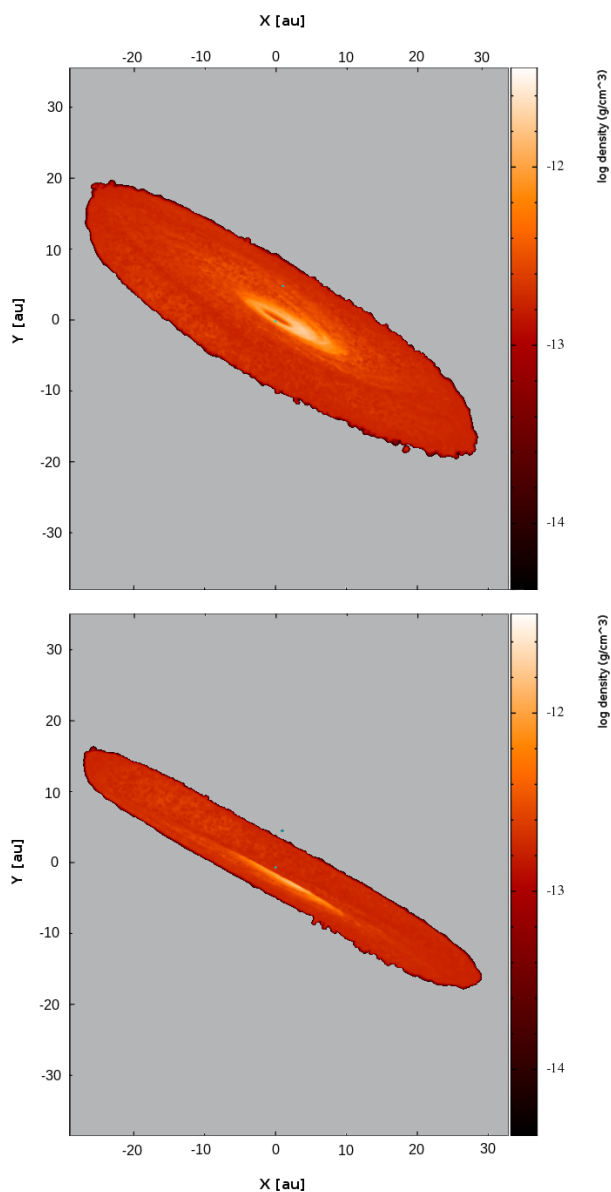


Fig. 1. 3D rendering of the disk + planet system in the *VINE* run. The plot is created through a ray tracing process, from an observer point of view placed at ~ 150 au from the disk. The disk is shown at an optical depth of ~ 2 , defined as the cross section per SPH particle mass.

negligible. Even in this case the planet decouple from the disk in a way very similar to that shown in Fig. 2 even if on slightly different timescales due to the different disk configuration and density. Initially, the smaller disk has a superficial density that is about 6 times higher compared to our standard disk. As a consequence, when the planet decouples from the disk, the repeated crossing of the disk plane lead to a different dynamical evolution since the frictional force depends on the local disk density. The increase of only 25% in the precession period of the disk initially extending over 15 au, instead of the expected factor 2 on the basis of eq. 3), is due to the radial spreading of the disk due to the strong binary perturbations. The standard disk with initial outer radius of about 30 au cannot spread beyond the tidal truncation limit and, as a consequence, its outer radius remains constant. On the other hand, the smaller disk has room to expand in response to the binary gravitational perturbations extending after one cycle (about 2×10^4 yr) beyond 25 au. The outcome of the

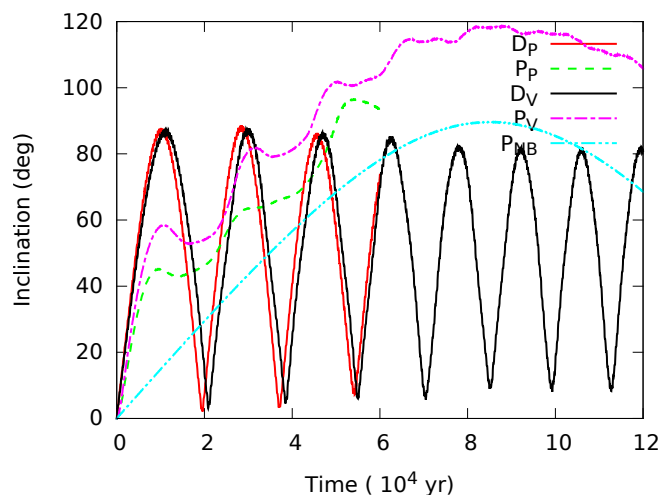


Fig. 2. Evolution of the disk and planet inclination respect to the initial disk+planet plane in the two runs with *VINE* and *PHANTOM*, respectively. The dashed magenta (*VINE*) and green (*PHANTOM*) lines show the planet inclination i_p while the continuous black (*VINE*) and red (*PHANTOM*) line illustrates the disk inclination i_d . After about 6000 yr, the planet evolution departs from that of the disk in both simulations and i_p grows at a slower rate compared to i_d . The light blue dashed-dotted line illustrates the evolution of the planet inclination in a pure N-Body problem Star-Planet-Companion star.

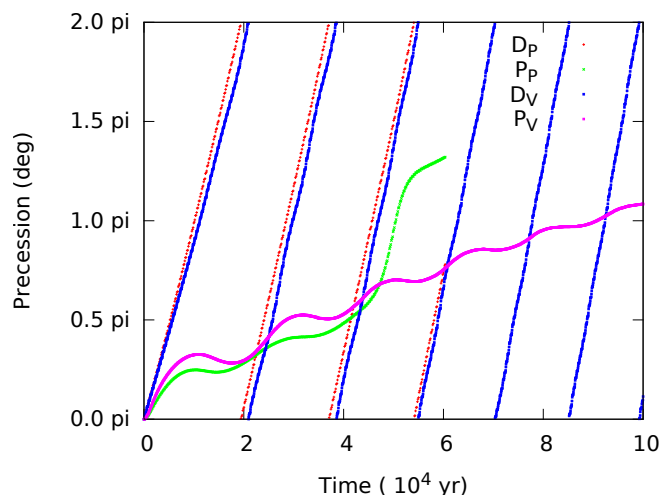


Fig. 3. Evolution of the disk and planet precession angle respect to the initial disk+planet plane, as defined in eq. 17. The dashed green line shows the planet precession angle β_p while the continuous red line illustrates the disk's one β_d .

numerical simulations rule out warping as responsible for the decoupling of a planet from its disk in our dynamical configuration since, according to (Terquem 2013), a severe warping is needed to affect the planet inclination. However, this mechanism may be an important one for closer binaries, increasing the decoupling rate between planet and disk.

The planet migration, in Fig. 6, is significantly slower compared to that found by (see Xiang-Grüss & Papaloizou 2014, Fig. 3). Apart from the initial fast migration rate when the planet is still embedded in the disk, when the planet detaches from the disk plane it is the friction developing during the periodic crossing of the disk by the planet that dominates the semimajor axis

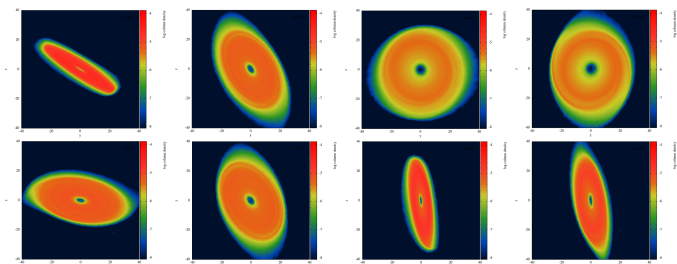


Fig. 4. Disk shape shown every 300 planetary orbits when the inclination of the planet is decoupling from that of the planet. The disk warping is negligible.

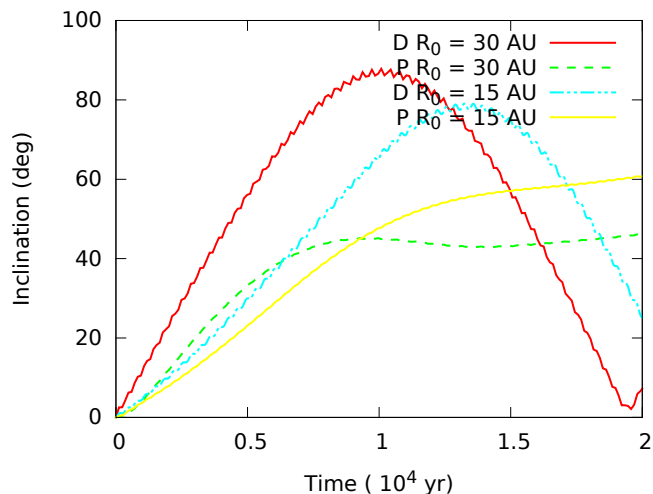


Fig. 5. Comparison of the planet and disk inclination evolution in the standard case, where the disk extends to 30 au, and a model with a smaller disk, extending to 15 au. No warping is expected in the latter case but the planet decouples from the disk as in our standard case with a larger disk.

evolution and migration. According to Teyssandier et al. (2013), the planet experiences a significant friction while crossing the disk due to aerodynamic drag and to a dynamical drag due to the gravitational scattering of the disk particles. The latter dominates since the ratio between the two friction forces can be expressed as (Teyssandier et al. 2013)

$$\frac{F_{\text{aer}}}{F_{\text{dyn}}} \sim \frac{1}{8 \ln\left(\frac{H(r)}{R_p}\right)} \left(\frac{R_p}{a}\right)^2 \left(\frac{M_s}{M_p}\right)^2 \quad (18)$$

where M_p and R_p are the mass and radius of the planet, respectively, and a is its semimajor axis. In our initial configuration where $a = 5$ au, $H(r) = h_s a \sim 0.19$ and assuming a radius of the planet $R_p \sim 2R_J \sim 0.001$ au we get a ratio lower than 0.02. In this situation the drag force is mostly due to the particle scattering during the planet crossing. There may also be an angular momentum exchange between the planet and the disk when the planet approaches the disk, but it has probably less effect on the long term drift.

The migration rate appears to be more irregular in the run with VINE respect to that with PHANTOM. This different behavior is possibly due to the mass accretion onto the planet in the PHANTOM run (the planet is modelled as a sink particle) which it is not implemented in the VINE run. In this last the planet cannot grow and gas is temporarily trapped and removed around it

during the disk crossing possibly leading to a noisy migration. In the run with PHANTOM, the planet has reached a mass of $1.6 M_J$ after about 4×10^4 yr and then the mass growth is reduced.

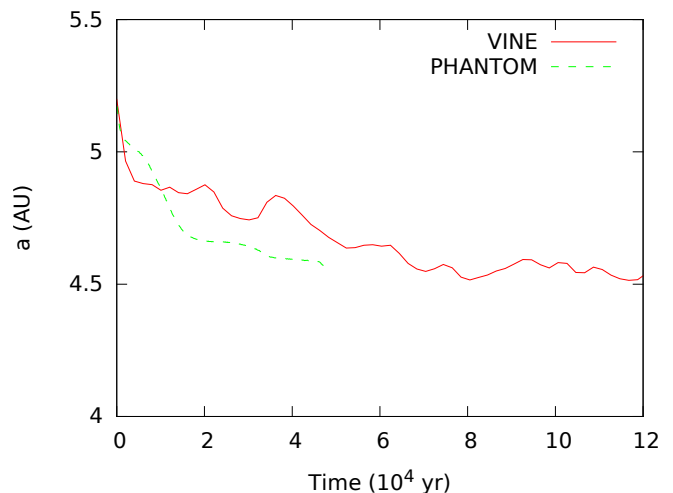


Fig. 6. Evolution of the semimajor axis of the planet in the VINE and PHANTOM runs, respectively. The planet migrates because of the friction with the gas when it periodically crosses the disk plane.

5. Initial mutual inclination of 60°

Even in the scenario with $i_B = 60^\circ$ we have run two different simulations, one with VINE and one with PHANTOM. In Fig. 7 we show the evolution of the disk and planet inclinations over a shorter timescale compared to the previous simulations where $i_B = 45^\circ$. However, it is already clear that the planet abandons the plane of the disk and evolves independently under the action of the companion star in both simulations. The disk influence appears to be a perturbing force also in this different scenario. The planet inclination, as in the $i_B = 45^\circ$, follows that of the disk only for a few 10^3 yr after which the planet detaches from the disk following an N-body behavior while the disk perturbs the dynamics especially when the planet crosses the disk. In the two models the planet evolution is different and this can possibly be ascribed to the diverse way of handling the gas trapped around the planet and to the different behavior of the disks in the two cases. After an initial quick increase of the disk inclination, the growth halts at about $i_d = 90^\circ$ and damped oscillations are thereafter observed in both cases. However, the increase in inclination appears more irregular in the run with VINE and stronger damped oscillations are observed immediately after the first maximum. In the run with PHANTOM, the evolution appears more regular and the damping more progressive. This different behavior may be ascribed to the different viscosity which seems to play a more relevant role on the evolution of the disk inclination when i_B is higher.

It is noteworthy that the damped oscillations recall, at some extent, those observed in Martin et al. (2014). However, the parameters of our model significantly differ from theirs so the exact same behavior is not expected. In particular, Martin et al. (2014) use 1) different temperature and density profiles, 2) their viscosity parameters are set in order to have a constant value of α_{SS} all over the disk, and 3) their disk is ten times less massive compared to ours. As a consequence, the evolution of the disk inclination is only qualitatively similar, but it is interesting that

in both scenarios damped oscillations are observed. An initial hint of damped oscillations of the disk inclination is also seen in the model with $i_B = 45^\circ$ (Fig. 2) even if, as already observed, it appears feeble.

A potential contribution to the strong damping in the $i_B = 60^\circ$ case is possibly related to the exchange of disk mass between the two stars. After about 2×10^4 yr from the beginning of the simulation the secondary star has gained a gaseous disk whose mass is about 5% that of the primary disk. The mass exchange is significantly lower in the $i_B = 45^\circ$ case where the acquired disk has a mass of only 0.05% of the initial disk mass. As a consequence, the viscosity of the disk plays a role also in an indirect way by forcing mass exchange for higher values of i_B leading to a damping of the disk inclination oscillations.

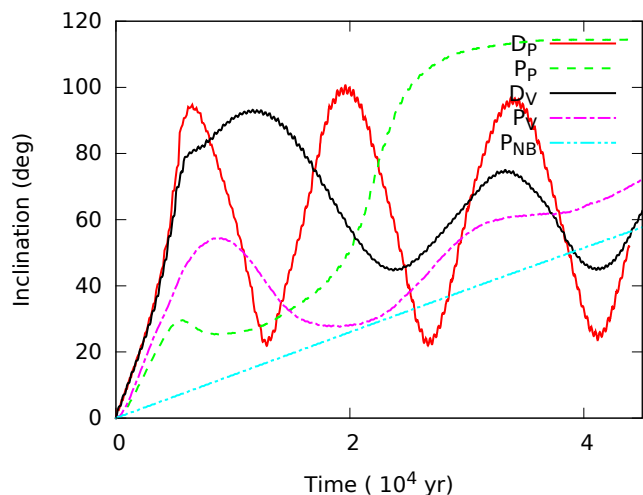


Fig. 7. Evolution of the disk and planet inclination respect to the initial disk+planet plane in the case with $i_B = 60^\circ$ in the *VINE* and *PHANTOM* runs, respectively. The symbols are the same as in Fig. 2.

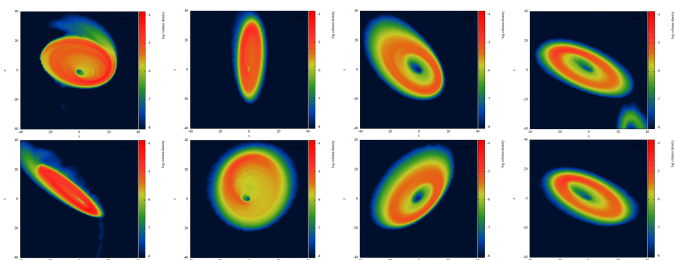


Fig. 8. Evolution with time of the disk in the *PHANTOM* model. Some mass leaves the primary disk and forms a ring around the secondary star. This behaviour was already observed in Picogna & Marzari (2013). No significant warping is observed.

Even in this case we tested the potential warping of the disk by plotting the disk evolution every 300 orbits of the planet. In this more inclined configuration we observe some mass transfer from the disk around the primary to the secondary star where a ring of gas slowly builds up. It is interesting to note that the disk eccentricity is higher compared to the case where $i_B = 45^\circ$ and comparable to that observed in Martin et al. (2014). This is why the mass flux from the primary towards the secondary star is more marked. In any case, the amount of mass extending out of the primary disk is not enough to cause a significant gravitational perturbation on the planet.

6. Discussion and Conclusions

We have shown that a Jupiter-like planet embedded in a circumstellar disk will evolve almost independently from the disk in response to the perturbations of a misaligned binary stellar companion for values of the semimajor axis a_B around 100 au. For inclinations of the binary plane of the order of 45° and 60° , after an initial coupled evolution, the planet dynamically detaches from the disk and its inclination oscillates on a significantly longer timescale compared to that of the disk. This occurs since the N-body secular perturbations of the companion star dominate over the damping force of the disk which tends to drag the planet back into its median plane. Our simulations have 3–times the resolution of those performed by Xiang-Gruess & Papaloizou (2014) and were performed with 2 different up to date SPH codes, *VINE* and *PHANTOM*.

Our results show that one of the fundamental requirements of the model of Batygin (2012) to explain the observed spin-orbit misalignment of some exoplanets is not met for small binary separations and a reasonable choice of physical parameters of the disk and planet. However, the migration of the planet appears to occur at a significant rate even if the orbit of the planet and the disk plane are not aligned. This is due to the friction with the gas during the repeated crossing of the disk by the planet. As a consequence, the inward drift of the planet would not be due to type I/II migration, as argued for wider separations by Crida & Batygin (2014), but to the dynamical friction with the disk. This would possibly lead to conclusions similar to those given in Batygin (2012) concerning the long term evolution of the planet spin axis and semimajor axis migration, but the physical mechanism would be different. The formation of hot Jupiters with spin misaligned respect to the stellar equator would in this case not occur because the planet follows the disk in its precession, but by a combination of N-body Kozai cycles and repeated crossing of the disk plane by the inclined planet evolving out of the disk. Even if the disk oscillations are damped over a long timescale to a given value of inclination, the continuous crossing of the disk by the planet following the Kozai-Lidov cycles would grant a significant migration.

Of course, a deeper exploration of the parameter space is needed to have a more complete scenario of the behavior of the system. We have also explored only one particular step of the system evolution while previous steps have also to be investigated. An example, when does the planet begin to evolve independently from its birth disk? At which stage of its growth? For which value of mass?

We have shown in our simulations that a Jupiter mass planet exits almost immediately from the disk, but does this occur also for smaller mass planets? Possibly not, since the final infall of gas on the planet core is a fast process occurring on a timescale shorter than the decoupling between the planet and disk inclination. However, the problem of growing a planet core in a disk perturbed by an inclined binary is a critical process. The condensation of dust into larger pebbles and, eventually, kilometer-sized planetesimals may be strongly perturbed in particular when the planetesimals decouple from the gas. For small inclinations between the circumprimary gas disk and the binary orbital plane Xie & Zhou (2009) and Xie et al. (2010) showed that planetesimal accretion may be fast because size segregation among planetesimals favors low velocity impacts. For larger inclinations, the nodal longitude randomization forced by the companion star may lead to the dispersion of the planetesimal disk reducing the chances of planet formation. However, Marzari et al. (2009b) showed that for binary semimajor axes larger than 70 au the

nodal longitude randomization timescale is longer than the planetesimal accretion process and core formation might occur. As a consequence, planet formation might occur within the disk even in presence of an inclined binary until the planet reaches a Jupiter mass or even more. After that, it would decouple from the disk and follow an independent evolution.

Additional simulations are needed to better explore the problem and different initial values have to be sampled for the planet mass, the binary orbital elements, and the disk parameters (like mass, viscosity, temperature distribution, density profile and so on) which can influence the propagation of perturbations. Running more numerical models may help to understand not only the response on the long term of the disk to the binary perturbations and the possible occurrence of damping, but also the dynamical evolution of the planet. The problem with these type of simulations is the large amount of CPU required by any run of an SPH code in this configuration.

Even if the migration of the planet in this scenario is due to the friction with the gas of the disk, it remains an open problem how to drive the planet very close to the star. Isothermal simulations of disks in binaries (Kley et al. 2008; Marzari et al. 2009a) show on the long term the formation of an elliptical hole in the density distribution close to the primary star. This would evidently halt the planet migration once the planet moves within the hole where either type I/II migration or, as we suggest in this paper, friction with the gas during the crossing of the disk would be switched off. However, more recent simulations with radiative disks do not show the formation of such an internal low density region (Müller & Kley 2012; Marzari et al. 2012; Picogna & Marzari 2013). This is an additional aspect that should be investigated to really understand the dynamical evolution of inclined hot Jupiters in misaligned binary star systems.

Acknowledgements. We thank an anonymous referee for his useful comments and suggestions. Many of our plots were made with the SPLASH software package (Price 2007). G. Picogna acknowledges the support through the German Research Foundation (DFG) grant KL 650/21 within the collaborative research program "The first 10 Million Years of the Solar System". Some simulations were performed on the bwGRiD cluster in Tübingen, which is funded by the Ministry for Education and Research of Germany and the Ministry for Science, Research and Arts of the state Baden-Württemberg, and the cluster of the Forschergruppe FOR 759 "The Formation of Planets: The Critical First Growth Phase" funded by the DFG.

References

Albrecht, S., Winn, J. N., Johnson, J. a., et al. 2012, *The Astrophysical Journal*, 757, 18
 Artymowicz, P. & Lubow, S. H. 1994, *The Astrophysical Journal*, 421, 651
 Artymowicz, P. & Lubow, S. H. 1996, *The Astrophysical Journal*, 467, L77
 Bate, M. R. 2000, *Monthly Notices of the Royal Astronomical Society*, 314, 33
 Bate, M. R., Bonnell, I. A., Clarke, C. J., et al. 2000, *MNRAS*, 317, 773
 Bate, M. R., Bonnell, I. A., & Price, N. M. 1995, *Monthly Notices of the Royal Astronomical Society*, 277, 362
 Batygin, K. 2012, *Nature*, 491, 418
 Bitsch, B. & Kley, W. 2011, *Astronomy & Astrophysics*, 530, A41
 Cresswell, P., Dirksen, G., Kley, W., & Nelson, R. P. 2007, *Astronomy & Astrophysics*, 473, 329
 Crida, A. & Batygin, K. 2014, *A&A*, 567, A42
 Daemgen, S., Correia, S., & Petr-Gotzens, M. G. 2012, *Astronomy & Astrophysics*, 540, A46
 Desidera, S. & Barbieri, M. 2007, *Astronomy & Astrophysics*, 462, 345
 Ford, E. B., Kozinsky, B., & Rasio, F. A. 2000, *ApJ*, 535, 385
 Kiseleva, L. G., Eggleton, P. P., & Mikkola, S. 1998, *MNRAS*, 300, 292
 Kley, W., Papaloizou, J. C. B., & Ogilvie, G. I. 2008, *A&A*, 487, 671
 Kozai, Y. 1962, *AJ*, 67, 591
 Lada, C. J. 2006, *The Astrophysical Journal Letters*, 640, L63
 Lai, D. 2014, *Monthly Notices of the Royal Astronomical Society*, 440, 3532
 Larwood, J. D., Nelson, R. P., Papaloizou, J. C. B., & Terquem, C. 1996, *Monthly Notices of the Royal Astronomical Society*, 282, 597

Lidov, M. L. 1962, *PSS*, 9, 719
 Lodato, G. & Price, D. J. 2010, *Monthly Notices of the Royal Astronomical Society*, 405, 1212
 Martin, R. G., Nixon, C., Lubow, S. H., et al. 2014, *ApJ*, 792, L33
 Marzari, F., Baruteau, C., Scholl, H., & Thebault, P. 2012, *A&A*, 539, A98
 Marzari, F. & Nelson, A. F. 2009, *The Astrophysical Journal*, 705, 1575
 Marzari, F., Scholl, H., Thébault, P., & Baruteau, C. 2009a, *A&A*, 508, 1493
 Marzari, F., Thébault, P., & Scholl, H. 2009b, *A&A*, 507, 505
 Meru, F. & Bate, M. R. 2012, *Monthly Notices of the Royal Astronomical Society*, 427, 2022
 Monaghan, J. J. 1997, *Journal of Computational Physics*, 136, 298
 Monaghan, J. J. & Gingold, R. A. 1983, *Journal of Computational Physics*, 52, 374
 Monin, J.-L., Clarke, C. J., Prato, L., & McCabe, C. 2007, *Protostars and Planets V*, 395
 Müller, T. W. A. & Kley, W. 2012, *A&A*, 539, A18
 Nelson, A. F., Wetzstein, M., & Naab, T. 2009, *The Astrophysical Journal Supplement Series*, 184, 326
 Papaloizou, J. C. B. & Terquem, C. 1995, *MNRAS*, 274, 987
 Pepliński, A., Artymowicz, P., & Mellema, G. 2008, *Monthly Notices of the Royal Astronomical Society*, 386, 164
 Picogna, G. & Marzari, F. 2013, *Astronomy & Astrophysics*, 556, A148
 Price, D. J. 2007, *PASA*, 24, 159
 Price, D. J. 2012, *Journal of Computational Physics*, 231, 759
 Price, D. J. & Federrath, C. 2010, *Monthly Notices of the Royal Astronomical Society*, 406, 1659
 Raghavan, D., McAlister, H. A., Henry, T. J., et al. 2010, *The Astrophysical Journal Supplement Series*, 190, 1
 Rein, H. 2012, *ArXiv e-prints [arXiv:1211.7121]*
 Rein, H. 2012, *Monthly Notices of the Royal Astronomical Society*, 422, 3611
 Reipurth, B. 2000, *The Astronomical Journal*, 120, 3177
 Roell, T., Neuhäuser, R., Seifahrt, A., & Mugrauer, M. 2012, *Astronomy & Astrophysics*, 542, A92
 Storch, N. I., Anderson, K. R., & Lai, D. 2014, *Science*, 345, 1317
 Terquem, C. 2013, *MNRAS*, 435, 798
 Teyssandier, J., Terquem, C., & Papaloizou, J. C. B. 2013, *Monthly Notices of the Royal Astronomical Society*, 428, 658
 Teyssandier, J., Terquem, C., & Papaloizou, J. C. B. 2013, *MNRAS*, 428, 658
 Thébault, P. & Haghighipour, N. 2014, in *Planetary Exploration and Science: Recent Advances and Applications*, 33
 Thommes, E. W. & Lissauer, J. J. 2003, *ApJ*, 597, 566
 Triud, A. H. M. J., Cameron, A. C., Queloz, D., et al. 2010, *Astronomy & Astrophysics*, 524, A25
 Wadsley, J. W., Veeravalli, G., & Couchman, H. M. P. 2008, *MNRAS*, 387, 427
 Wetzstein, M., Nelson, A. F., Naab, T., & Burkert, A. 2009, *The Astrophysical Journal Supplement Series*, 184, 298
 Xiang-Gruess, M. & Papaloizou, J. C. B. 2013, *Monthly Notices of the Royal Astronomical Society*, 431, 1320
 Xiang-Gruess, M. & Papaloizou, J. C. B. 2014, *Monthly Notices of the Royal Astronomical Society*, 440, 1179
 Xie, J.-W. & Zhou, J.-L. 2009, *ApJ*, 698, 2066
 Xie, J.-W., Zhou, J.-L., & Ge, J. 2010, *ApJ*, 708, 1566